The Journal of Immunology

Labile Zinc and Zinc Transporter ZnT_4 in Mast Cell Granules: Role in Regulation of Caspase Activation and NF-κB Translocation

Lien H. Ho, Richard E. Ruffin, Chiara Murgia, Lixin Li, Steven A. Krilis and Peter D. Zalewski

J Immunol 2004; 172:7750-7760; ;
doi: 10.4049/jimmunol.172.12.7750
http://www.jimmunol.org/content/172/12/7750

The Journal of Immunology is published twice each month by
The American Association of Immunologists, Inc.,
1451 Rockville Pike, Suite 650, Rockville, MD 20852

Print ISSN: 0022-1767 Online ISSN: 1550-6606.

Labile Zinc and Zinc Transporter ZnT_4 in Mast Cell Granules: Role in Regulation of Caspase Activation and NF-κB Translocation[1]

Lien H. Ho,* Richard E. Ruffin,* Chiara Murgia,† Lixin Li,‡ Steven A. Krilis,‡ and Peter D. Zalewski[2]*

The granules of mast cells and other inflammatory cells are known to be rich in zinc (Zn), a potent caspase inhibitor. The functions of granular Zn, its mechanism of uptake, and its relationship to caspase activation in apoptosis are unclear. The granules of a variety of mast cell types fluoresced intensely with the Zn-specific fluorophore Zinquin, and fluorescence was quenched by functional depletion of Zn using a membrane-permeable Zn chelator *N*, *N*, *N′*, *N′*-tetrakis (2-pyridyl-methyl)ethylenediamine (TPEN). Zn levels were also depleted by various mast cell activators, including IgE/anti-IgE, and Zn was rapidly replenished during subsequent culture, suggesting an active uptake mechanism. In support of the latter, mast cells contained high levels of the vesicular Zn transporter ZnT_4, especially in the more apical granules. Immunofluorescence and immunogold labeling studies revealed significant pools of procaspase-3 and -4 in mast cell granules and their release during degranulation. Functional depletion of Zn by chelation with TPEN, but not by degranulation, resulted in greatly increased susceptibility of mast cells to toxin-induced caspase activation, as detected using a fluorogenic substrate assay. Release of caspases during degranulation was accompanied by a decreased susceptibility to toxins. Zn depletion by chelation, but not by degranulation, also resulted in nuclear translocation of the antiapoptotic, proinflammatory transcription factor NF-κB. These findings implicate a role for ZnT_4 in mast cell Zn homeostasis and suggest that granule pools of Zn may be distinct from those regulating activation of procaspase-3 and NF-κB. ***The Journal of Immunology*****, 2004, 172: 7750–7760.**

Mast cells are granulated cells that are especially localized within connective tissues and epithelial surfaces, and that play an important role in the inflammatory and immune systems (1). Regulation of their numbers is largely dependent upon proliferative and/or apoptotic signals (2). It has been shown that mouse mast cells undergo apoptosis as a result of IL-3 withdrawal, and this coincides with a decrease in endogenous *bcl*-2 mRNA (2). This effect was reversible upon addition of stem cell factor (SCF).[3] Although mast cells can recover their content of histamine and other granule components after degranulation (3), it is not clear whether this process makes them more susceptible to apoptosis.

Electron microscopic studies in the 1960s demonstrated that mast cell granules were rich in zinc (Zn) (4). Although this Zn may play a role in storage of granule contents, other functions may exist. Our previous studies using a Zn-specific fluorophore Zinquin have revealed the presence of discrete vesicular pools of free or loosely bound (labile) Zn in a variety of cell types (5, 6) and a cytoprotective role for this Zn via the regulation of activation of procaspase-3, the zymogen form of a major effector of apoptosis (7, 8).

Another important question concerns the mechanism by which mast cells accumulate Zn and transport it into secretory granules. In mammals, two families of genes coding for Zn transporters have been identified and cloned. The members of the hZIP family have been shown to mediate uptake of Zn across the plasma membrane, analogous to the ZRT1/ZRT2 Zn uptake transporters in yeast (9–11). The proteins belonging to the second group, cation diffusion facilitator, are all involved in Zn efflux or intracellular sequestration in vesicles. In mammals, this family comprises at least seven proteins: ZnT_1 is a plasma membrane efflux transporter that was shown to confer Zn resistance to cells (9); ZnT_2 and ZnT_4 are localized in cell vesicles (10, 11); ZnT_3, which is expressed mainly by neuronal cells, incorporates Zn into vesicles at neuronal presynaptic terminals (12); ZnT_5 is thought to transport Zn into insulin-containing secretory granules of pancreatic β cells (13) and is involved in the intestinal absorption of Zn (14); ZnT_6 and ZnT_7 were recently identified by virtue of their homology to ZnT_4 and ZnT_1, respectively, from the expressed sequence tag database (9). A point mutation in ZnT_4 represents the molecular basis of the murine syndrome lethal milk that determines a defect in Zn secretion in milk (15). The corresponding gene is widely expressed in tissues (16), suggesting a potential role for this protein in the secretion of Zn in other cell systems. There has been no study of Zn transporters in mast cells.

An important factor mediating the suppression of apoptosis in inflammatory cells is the transcription factor NF-κB. NF-κB

*Department of Medicine, University of Adelaide, The Queen Elizabeth Hospital, Woodville, South Australia; †Istituto Nazionale Ricerca per gli Alimenti e la Nutrizione, Rome, Italy; and ‡Department of Immunology, Division of Medicine, University of New South Wales, St. George Hospital, Sydney, New South Wales, Australia

Received for publication May 29, 2003. Accepted for publication April 1, 2004.

The costs of publication of this article were defrayed in part by the payment of page charges. This article must therefore be hereby marked *advertisement* in accordance with 18 U.S.C. Section 1734 solely to indicate this fact.

[1] This work was, in part, presented at the European Respiratory Society Conference in Florence, Italy (September 2000).

[2] Address correspondence and reprint requests to Dr. Peter D. Zalewski, Department of Medicine, University of Adelaide, 5th Floor 5B, The Queen Elizabeth Hospital, Woodville, South Australia, Australia 5011. E-mail address: peter.zalewski@adelaide.edu.au

[3] Abbreviations used in this paper: SCF, stem cell factor; CBMC, cord blood mast cell; GSU, gray scale unit; HMC, human mast cell line; MDCK, Madin-Darby canine kidney; RPMC, rat peritoneal mast cell; RT, room temperature; TPEN, *N*,*N*,*N′*, *N′*-tetrakis(2-pyridyl-methyl)ethylenediamine; Zn, zinc.

0022-1767/04/$02.00

regulates the expression of a broad range of genes involved in inflammatory diseases (17), as well as regulating the apoptosis process (18). Although some evidence has been presented suggesting that NF-κB is proapoptotic, the bulk of evidence supports the hypothesis that NF-κB is antiapoptotic and prolongs the survival of inflammatory cells (19). Therefore, it was of interest to determine whether Zn influences activation of NF-κB in mast cells.

Zn has been depleted from cells in vitro by a range of techniques (5), including culture in Zn-free medium and use of membrane-permeable Zn chelators such as 1, 10 phenanthroline and *N*,*N*,*N*′,*N*′-tetrakis(2-pyridylmethyl)ethylendiamine (TPEN). Depletion of intracellular Zn in the experiments described in this work was induced by TPEN because it acts more rapidly than by culturing in Zn-free medium and its action is more specific than that of phenanthroline. Various methods have been used to increase intracellular Zn. These include addition of high concentrations of Zn salts to the medium or the use of lower concentrations of Zn salts in the presence of Zn ionophores, such as di-iodoquinoline and sodium pyrithione. The latter act more rapidly to increase intracellular Zn levels than by exposing cells to $ZnSO_4$ alone and avoid the use of very high extracellular Zn concentrations, which may be toxic to cells (5).

This study therefore aimed to investigate levels and distribution of labile Zn in mast cells, and to correlate with ZnT_4, procaspase-3, and NF-κB, before and after activation-induced degranulation. Labile Zn was quantified using the Zn-specific fluorophore Zinquin and image analysis. Changes in procaspase-3 were compared with those of procaspase-4, which is largely involved in proinflammatory events (20). Activation of NF-κB was determined by immunofluorescence labeling and nuclear translocation. Experiments were performed in the human mast cell line (HMC-1), either before or after maturation overnight with 1 mM sodium butyrate (21, 22), as well as in a variety of types of primary human and rat mast cells. At this concentration, butyrate is an effective inducer of maturation in a number of diverse cell types (discussed in Ref. 23). Higher concentrations of butyrate (4 mM and greater) induce apoptosis in various types of cell (23) and were used in this work to induce procaspase-3 activation and apoptosis in mast cells. Butyrate is thought to induce a novel pathway of caspase-3 activation and apoptosis that is dependent on inhibition of histone deacetylase and new protein synthesis (23). In addition, the protein kinase inhibitor staurosporine was used as a trigger for apoptosis, because this agent acts differently from, and synergistically with, butyrate in induction of caspase-3 activation (23).

Materials and Methods

Materials

Major materials and their suppliers were: BSA, A23187, diothiothrietol, EDTA, DNP-IgE, DNP-BSA, glutaraldehyde, Hoechst dye 33342, PMA, metrizamide, Nonidet P-40, human IgE, mouse IgG, human rSCF, rIL-6, HEPES, paraformaldehyde, sucrose, TPEN, and Triton X-100 (Sigma-Aldrich, St. Louis, MO); sodium butyrate (BDH, Poole, U.K.); penicillin/streptomycin, RPMI 1640, Histopaque, EDTA/trypsin, glutamine, and CHAPS (ICN Pharmaceuticals, Aurora, OH); FBS (BD Biosciences, Sydney, Australia); gentamicin (David Bull Labs, Melbourne, Victoria, Australia); rabbit anti-human IgE (DAKO, Botany, New South Wales, Australia); DEVD-AFC (Kamiya Biomedical, Tukwila, WA). Zinquin, ethyl-[2-methyl-8-*p*-toluenesulphonamido-6-quinolyloxy]acetate was obtained from A. Ward (Department of Chemistry, University of Adelaide). It was dissolved in DMSO at 5 mM and stored at −20°C in the dark. TPEN was stored at −20°C as a stock solution (5 mM) in DMSO. All other reagents were reagent grade.

Cell culture

Unless otherwise indicated in text, all cells were cultured in a humidified atmosphere containing 5% CO_2 in RPMI 1640, HEPES buffered, pH 7.4, supplemented with glutamine (2 mM), penicillin (100 IU/ml), streptomycin (100 μg/ml), gentamicin (160 μg/ml), and 10% FBS (complete medium). Experiments were performed either in 25-cm^2 vented tissue culture flasks (Iwaki, Funabasi, Chiba, Japan) or six-well plates (Falcon; BD Labware, Franklin Lakes, NJ). Viability was monitored by trypan blue exclusion. Metachromatic granule-containing cells were identified by staining with 1% toluidine blue in methanol, pH 2.5.

Cell lines

HMC-1 was obtained from J. Butterfield (Division of Allergy and Outpatient Infectious Diseases, Mayo Clinic and Foundation, Rochester, MN). Maturation was achieved by treatment with 1 mM sodium butyrate for 4 days under normal culture conditions (21, 22). These cells are referred to as mature HMC-1 cells. RBL-2H3 rat basophilic mast cell line was from R. Ludowyke (Centre for Immunology, St. Vincent's Hospital, University of New South Wales, Sydney, Australia). A549 cells were obtained from D. Knight (QE II Medical Center, University of Western Australia, Nedlands, Australia). A549 cells were derived from a human alveolar cell carcinoma; they are epithelial in morphology, hyperdiploid, and represent alveolar epithelial cells (24).

Primary mast cell cultures

Cord blood mast cells (CBMC) were isolated from umbilical cord blood by Histopaque density centrifugation (density 1.077 g/ml) (25). Cells at the interface were collected, washed three times with PBS, and cultured for 5 wk in complete medium, further supplemented with 100 ng/ml SCF and 50 ng/ml IL-6. CBMC were purified using mAb YB5.B8 (a gift from L. Ashman, Institute of Veterinary Science, Adelaide, Australia) using an immunobead selection method previously described (26). Dynabeads were coated with sheep anti-mouse IgG (Dynal Biotech, Gosford, New South Wales, Australia) for 1 h with gentle shaking (Dynabead:CBMC ratio = 6:1).

Peritoneal mast cells (RPMC) were isolated from 6- to 8-wk-old female 180 g Dark Agouti rats. Twenty milliliters of cold Tyrode's buffer (140 mM NaCl, 3 mM KCl, 0.4 mM NaH_2PO_4, 2 mM $CaCl_2$, 1 mM $MgCl_2$, and 6 mM glucose, pH 7.4) were injected into the peritoneal cavity, and the abdomen was massaged for 2 min. A small incision was then made at the lower midline of the peritoneal lining to open the cavity, and a sterile pasteur pipette was used to collect the peritoneal wash. RPMC were centrifuged at 150 × *g* for 10 min at room temperature (RT), and the cell pellet was resuspended in 1 ml of Tyrode's buffer per rat. RPMC were layered on 2 ml of 22% metrizamide and centrifuged at 280 × *g* for 15 min at RT. The pellet was resuspended in 20 ml of Tyrode's buffer and centrifuged at 150 × *g* for 10 min at RT. The metrizamide step was repeated, and the lower third of the gradient containing purified mast cells was collected. Isolated cells were washed once more with Tyrode's buffer. Bone marrow-derived mast cells were obtained from normal donors according to the protocol described in Li et al. (27).

There were some limitations that precluded all experiments being conducted on each of the cell types, especially primary mast cells.

Alteration of levels of intracellular Zn

Intracellular Zn was depleted from cells using TPEN. TPEN is a selective chelator of transition metals due to the pyridines groups acting as soft electron donors. It has a very high affinity for Zn (log K = 15.58) as well as iron (log K = 14.61), but has negligible affinity for calcium and magnesium (log K = 4.4 and 1.7, respectively) (28). In these experiments, supplementation of cells with Zn was accomplished by addition of 25 μM $ZnSO_4$ and sodium pyrithione (4 μM, unless otherwise indicated). Pyrithione forms lipophilic complexes with Zn; it also binds nickel and cadmium ions (neither of which is present in significant concentrations in biological tissues), but does not bind or transport calcium or magnesium ions (29).

Zinquin fluorescence image analysis

To investigate the levels and distribution of labile Zn in mast cells, the membrane-permeant Zn-specific fluorophore Zinquin was used. Under UV light (excitation λ 364 nm), Zinquin-Zn complexes emit a vivid blue fluorescence (peak emission λ 485 nm), giving a stable signal in intact cells and tissues (5). It does not fluoresce with other metal ions, except for a weak reaction with cadmium (6). Zinquin forms two complexes with Zn with stability constants of 2.7×10^6 dm^3mol^{-1} (1:1 complex) and 11.7 ×

10^6 dm^3mol^{-1} (2:1); these relatively low affinities for Zn ensure that Zinquin preferentially reacts with the most labile Zn pools in a range of cell types and tissues (5–7, 30).

RBL-2H3 cells were grown on poly(L-lysine)-coated glass coverslips, while other cells were labeled as wet suspensions. Cells were incubated with 25 μM Zinquin for 30 min at 37°C. For video image analysis, cells were examined using an Olympus epifluorescence microscope, equipped with a UV-B dichroic mirror for low wavelength excitation, and connected to a CCTV video color camera and computer work station. Images were captured and fluorescence was quantified using the Video Pro Image Analysis System (Leading Edge, Marion, South Australia.). For confocal microscopy, a Bio-Rad (Hercules, CA) MRC-1000 laser scanning confocal microscope system, equipped with a UV-Argon laser, was used in combination with a Nikon Diaphot 300 inverted microscope in fluorescence mode with excitation at 363/8 nm and emission at 460 LP. Images were collected using ×40 water immersion objective lens with NA 1.15. Each image was averaged over six scans by Kalman filtering.

Expression of ZnT_4 by RT-PCR

Method for RT-PCR was described previously (10). cDNA was prepared from 1 μg of total RNA using reverse transcriptase (Moloney murine leukemia virus; Invitrogen-Life Technologies, Carlsbad, CA) and random hexamer primers. First strand cDNA was PCR amplified with polyTaq enzyme, using the following oligonucleotides as primers: ZnT_4 sense, ATGGGCAGGGACGCGCCGGCCTG; ZnT_4 antisense, GTACTGGAA CTTTGACAATTTGCACA; hGAPDH sense, AAACCCATCACCATCT TCCAG; hGAPDH antisense, AGGGGCCATCCACAGTCTTCT; rat

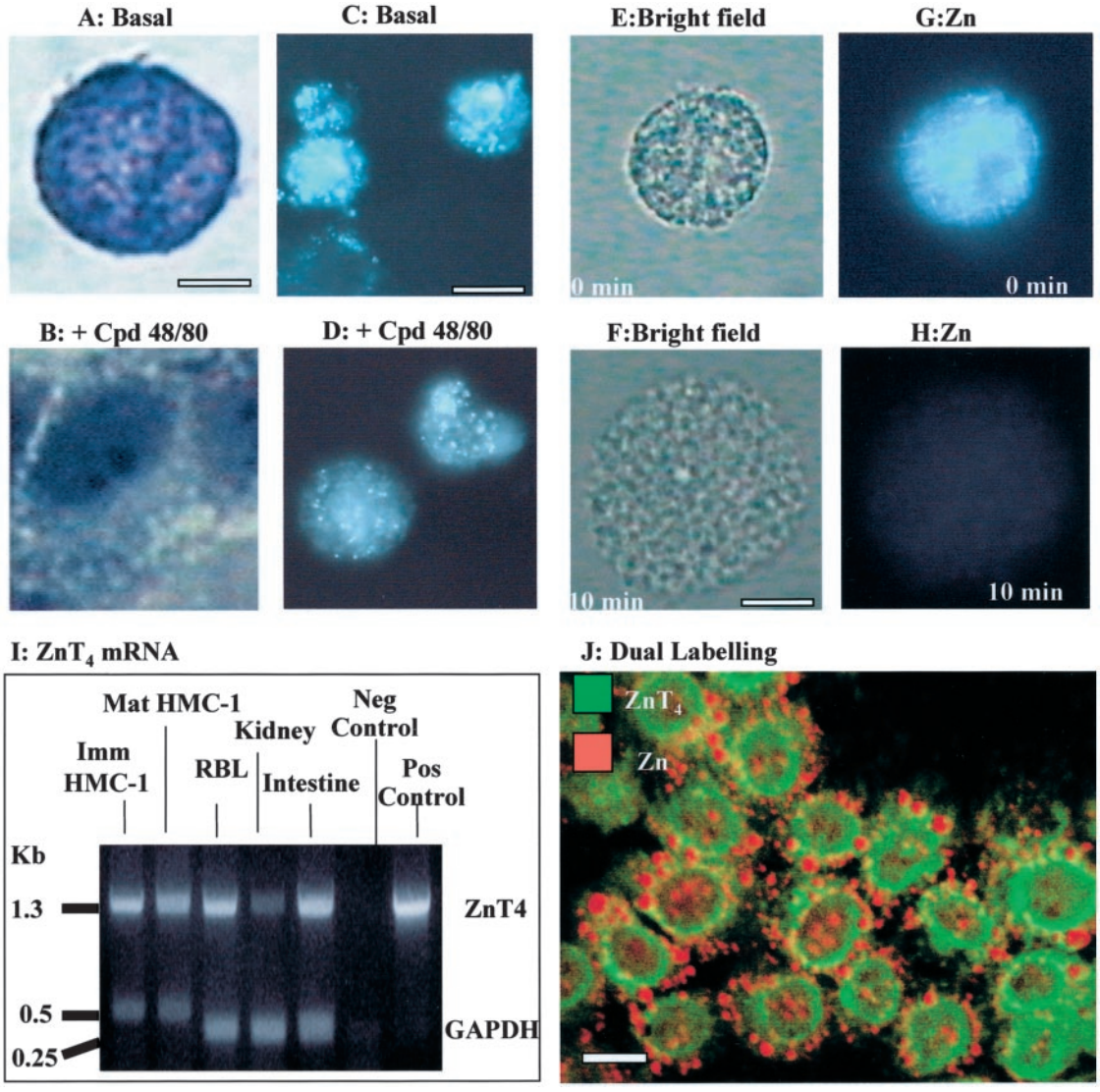

FIGURE 1. Zn and ZnT4 in untreated and activated mast cells. *A–D*, Show the decrease in Zinquin fluorescence and corresponding toluidine blue staining for HMC-1 mast cells before (*A* and *C*) and after (*B* and *D*) treatment with compound 48/80 for 18 h. *A*, Shows a typical mature mast cell in which the granules are densely stained with toluidine blue. *B*, Shows vacuolation and diffuse pale toluidine blue staining, indicating loss of granules. *C*, Shows intense particulate Zinquin fluorescence labeling, demonstrating presence of large amounts of Zn within the granules. *D*, Shows partial loss of Zinquin labeling in degranulated mast cells. The scale bar indicates 6 μm in *A* and *B*, and 14 μm in *C* and *D*. *E–H*, Time-lapse images of an RPMC undergoing UV-induced degranulation (*E* and *F*, bright field images) and loss of Zn (*G* and *H*, corresponding UV fluorescence) at 10 min. Note the increase in surface area due to swelling of granules and the marked reduction in Zn-dependent Zinquin fluorescence (*F* and *H*). The scale bar indicates 7 μm in *E–H*. *I*, A typical RT-PCR of mRNA in immature HMC-1 mast cells (Imm), mature HMC-1 mast cells (Mat), RBL mast cells, rat kidney, rat intestine, or positive control (antisense primer derived from the coding sequences of ZnT_4). Primers specific for the housekeeping enzyme GAPDH were included as internal control. The negative control contained RNA from extracts not exposed to reverse-transcriptase enzyme. For convenience, the negative control using intestinal extract is shown. Figure shows high expression of ZnT_4 mRNA in each mast cell type, comparable to the high levels found in intestine. *J*, Dual immunofluorescence and Zinquin labeling in mature HMC-1 cells by confocal microscopy, showing only partial colocalization of ZnT_4 (green) vesicles and Zn-containing vesicles (red). Scale bar indicates 12 μm.

GAPDH sense, GCCATCAACGACCCCTTCAT; and rat GAPDH antisense, CGCCTGCTTCACCACCTTC. Primers specific for the housekeeping enzyme GAPDH were included as internal control. A negative control containing RNA from extracts lacking treatment with reverse transcriptase was used to exclude contamination of genomic DNA in the samples.

Detection of ZnT_4 and procaspase-3 mRNA by Northern hybridization

Methods were described previously (10, 16). Positive controls were the Madin-Darby canine kidney II cells (MDCK II) transfected with the full length of rat ZnT_4-*myc* cDNA and cultured in medium lacking doxycycline (MDCK II Dox^-). The negative control was transfected MDCK II cells cultured in medium in the presence of doxycycline (MDCK II Dox^+). MDCK II Dox^+ expresses little or no ZnT_4. Equal loading was assessed by ethidium bromide staining of 18S rRNA (10). Band intensities were quantified using a phosphor imager (FujiFilm BAS-1500) and expressed as arbitrary units.

A similar method was used for detection of human procaspase-3 in mast cells. Human procaspase-3 insert and controls were a gift of P. Cowled (Queen Elizabeth Hospital, Adelaide, Australia). Positive control was mRNA from SW620 cells.

Immunofluorescence labeling of procaspase-3 and -4

Cytospins of mast cells were air dried for 20 min and fixed in 4% paraformaldehyde in PBS for 30 min at RT. Cells were washed twice in cold PBS and permeabilized with 0.2% Triton X-100 in PBS for 10 min at −20°C, then washed twice again in cold PBS. Cells were incubated in 1% BSA + PBS for 20 min at RT, followed by two washes in cold PBS. Cytospins were labeled with a polyclonal rabbit anti-human caspase-3 (1/100 dilution; BD PharMingen, Bedford, MA) for 18 h at RT. These were then washed three times with 1% BSA + PBS and twice with cold PBS and incubated with a FITC-conjugated goat anti-rabbit IgG (1/100 dilution; Rocklands, Gilbertsville, PA) for 2 h at RT. Cells were washed, mounted, and visualized under epifluorescence or confocal fluorescence microscopy. The same protocol was performed for staining of caspase-4 using primary polyclonal goat anti-caspase-4 Ab (1:100; Santa Cruz Biotechnology, Santa Cruz, CA) and secondary FITC-conjugated bovine anti-goat IgG (1/100; Santa Cruz Biotechnology).

NF-κB immunofluorescence and nuclear translocation

For NF-κB labeling, cells were stimulated with 20 ng/ml TNF-α or other agents, as indicated. Cytospins were pretreated with 0.05% Tween 20 + 3% BSA in PBS for 20 min at RT, followed by two washes in cold PBS for 2 min each, before addition of rabbit polyclonal IgG against the p65 subunit of NF-κB (1/20 dilution; Santa Cruz Biotechnology) at RT for 18 h. Cells were washed three times with cold 1% BSA + PBS for 3 min each at RT, followed by two washes with cold PBS for 2 min each at RT. FITC-conjugated goat anti-rabbit IgG was then added for a further 1.5 h at RT. After the incubation, cells were washed with 1% BSA + PBS and cold PBS, as described above. Measurements were performed blinded.

Dual labeling of ZnT_4 and Zn

For dual labeling studies of ZnT_4 and Zn, a similar protocol was used for that of procaspase-3, except that, after secondary Ab addition, cells were dual labeled for Zinquin, as described below. Triton X-100 permeabilization does not interfere with Zinquin fluorescence in paraformaldehyde-fixed cells. Specificity for Zinquin is shown by quenching of fluorescence in the presence of 25 μM TPEN. Primary Ab was rabbit anti-rat ZnT_4 (1/250 dilution) (16) for 18 h at RT, and secondary Ab was FITC-conjugated goat anti-rabbit IgG (1/250 dilution; Rocklands) for 2 h at RT. Slides were washed and Zinquin was added to a final concentration of 25 μM in PBS. Cells were examined by confocal microscopy. Images were collected and merged to study colocalization of Zn and ZnT_4.

Immunogold labeling of procaspase-3 and ZnT_4

Mast cells were fixed in 0.25% glutaraldehyde, 4% paraformaldehyde in PBS with 4% sucrose, pH 7.2, for 1 h at RT. Cells were washed in PBS + 4% sucrose, followed by a wash in 50% ethanol for 30 min, then 70% ethanol for 1 h. Cells were then placed in a 1:1 mix of 70% ethanol and LR White resin (ProSciTech, Thuringowa, Queensland, Australia) for 1 h at RT, followed by a 1:2 mix of 70% ethanol and LR White resin for 1 h at RT. Cells were embedded in LR White resin for 1 h at RT, followed by three changes of resin and concentration in a gelatin capsule that was incubated at 50°C overnight. Sections of 70 nm were placed onto nickel-coated grids, immersed in glycine solution, followed by a 1% BSA solution in PBS containing 0.5% Tween 20 and 0.1% Triton X-100 for 20 min. These were dried and incubated with primary Ab at 1/100 dilution as for immunofluorescence. Grids were washed in PBS and incubated with gold-labeled goat anti-rabbit IgG (1/100, 10 nm; Aurion, Wageningen, The Netherlands). Grids were washed in PBS and distilled water, before staining with uranyl acetate and lead citrate.

Fluorogenic substrate assay for caspase-3

Caspases-3 was assayed by cleavage of fluorogenic substrate zDEVD-AFC (z-asp-glu-val-asp-7-amino-4-methyl-coumarin), as described previously (23).

Hoechst dye 33342 staining of chromatin

To confirm apoptosis in some experiments, cells were incubated with Hoechst dye 33342 (final concentration of 1 μg/ml) for 10 min and examined by epifluorescence microscopy. Cells were classified according to whether there were homogenous nuclear staining (no apoptosis), nuclear rim of condensed chromatin (early stage of apoptosis), or fragmented chromatin (late stage of apoptosis). These measurements were performed blinded.

Experimental analysis

Data are expressed as mean ± SEM. Significances were determined by Student's *t* test, except for data (see Table III) in which one-way ANOVA analysis was used in conjunction with the post hoc Tukey-Honestly Significantly Different test. Values of *p* are shown: *, $p < 0.05$; **, $p < 0.005$. All protocols involving human tissues were approved by the North Western Adelaide Health Service Ethics of Human Research Committee. Animal experiments were approved by the North Western Adelaide Health Service Ethics of Animal Research Committee.

Results

Zinquin fluorescence of mast cells before and after degranulation

Mast cells fluoresced intensely when labeled with Zinquin, suggesting high levels of labile Zn. This can be seen by comparison

Table I. *Effects of treatment with activators or TPEN on Zinquin fluorescence of mast cells*

Mast Cell Type	Treatment[a]	Zinquin Fluorescence[b] (% of control, ± SEM)
Immature HMC-1	48/80 (1 μg/ml)	59.5 ± 6.1**
	IgE (5 μg/ml) + anti-IgE (0.2 μM)	58.4 ± 7.1*
	TPEN (50 μM)	39.4 ± 7.6**
Mature HMC-1	48/80 (1 μg/ml)	55.9 ± 2.8**
RPMC	48/80 (1 μg/ml)	35.2 ± 1.5**
Bone marrow derived	IgE (5 μg/ml) + anti-IgE (0.2 μM)	65.8 ± 9.4*
	PMA (100 nM) + A23187 (0.5 μM)	41.4 ± 27.7*
	TPEN (100 μM)	53.7 ± 6.8**
CBMC	48/80 (1 μg/ml)	49.1 ± 2.5**

[a] Cells were treated for 18 h at 37°C with reagents in culture medium, except for TPEN, which was added for 2 h.
[b] Zinquin fluorescence of cells expressed as percentage of fluorescence of control cells.
At least 20 cells were quantified by image analysis from replicate tubes. *, $p < 0.05$; **, $p < 0.005$.

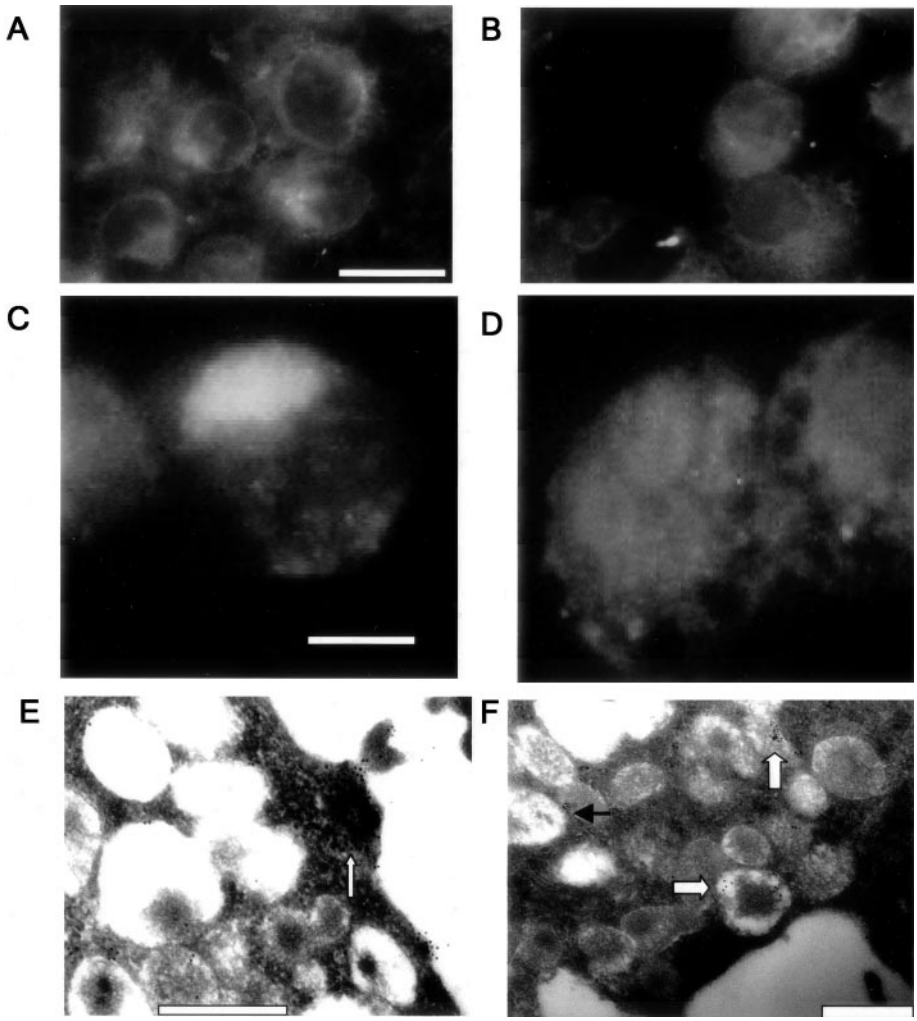

FIGURE 2. Expression and localization of ZnT4 in mast cells. *A–D*, Show ZnT_4 immunofluorescence in immature HMC-1 cells or RPMC before (*A* and *C*) and following (*B* and *D*) activation with 1 μg/ml compound 48/80 for 18 h at 37°C. Scale bar indicates 16 μm in *A* and *B*, and 6 μm in *C* and *D*. Note the strong apical fluorescence in *C*. *E* and *F*, Show immunogold labeling of ZnT_4 in immature HMC-1 cells, especially inside of granules (thick open arrows), lining the granules (filled arrow), and in the surrounding cytoplasm (thin open arrows). Scale bars indicate 500 nm.

with the human lung epithelial cell line A549, typical of many other types of cell studied. At the same microscope and lamp settings, A549 cells had a weak fluorescence, of 10.1 ± 0.6 gray scale units (GSU), while human CBMC had 80.5 ± 4.5, immature HMC-1 had 132.4 ± 11.1, and RBL-2H3 had 60.4 ± 3.0. In separate experiments (data not shown), similar intense Zinquin fluorescence was seen with mature HMC-1 cells, RPMC, and bone marrow-derived mast cells. Fluorescence of untreated mast cells was largely cytoplasmic with a pronounced granular-like distribution (Fig. 1*C*), suggesting that the bulk of Zn may be within secretory granules of these cells. There was no significant difference in Zinquin fluorescence between immature HMC-1 and mature HMC-1, suggesting that Zn levels do not change with butyrate-induced maturation (data not shown). The criteria for maturation were increased granularity assessed by staining of granules with toluidine blue and by electron microscopy (22). Different types of granules were seen at higher magnification in the mature HMC-1 cells. These included granules with a scroll-like pattern and amorphous granules with various amounts of electron-dense material. Zinquin fluorescence was quenched by the Zn chelator TPEN, confirming that the fluorescence was due to Zn. For example, 50 μM TPEN decreased Zinquin fluorescence of immature HMC-1 cells by 60.6 ± 7.6% ($p < 0.005$).

Fig. 1 shows numerous granules in mature HMC-1 mast cells stained with toluidine blue (Fig. 1*A*) and labeled with Zinquin (Fig. 1*C*). To confirm that Zinquin-detectable Zn was within the granules, mast cells were induced to degranulate by treatment with 1 μg/ml compound 48/80 for 18 h at 37°C. Degranulation was confirmed by the appearance of a pale vacuolated cytoplasm, accompanied by an increase in cell size (Fig. 1*B*). Following degranulation with compound 48/80, the mean area of mature HMC-1 cells increased by 69 ± 3.1% and the mean area of immature HMC-1 cells increased by 66.4 ± 2.7%.

Accompanying morphological changes, there was a significant decrease in Zinquin labeling in the degranulated cells (Fig. 1*D*). A similar loss of Zn was seen in RPMC undergoing UV-induced degranulation over a time period of 10 min (Fig. 1, *E–H*). In the latter experiment, degranulation was triggered in ~5% of the cells by exposure on microscope slides to UV light from a fluorescence microscope equipped with argon lamp and UV-B excitation filter. Accompanying degranulation, there was a 2- to 3-fold increase in cell volume, evidence of membrane and granule swelling, and extensive puffing at the cell surface, typical of cells undergoing exocytosis. UVB light is a known inducer of degranulation in RPMC, and this process is independent of significant cell death or lysis (31). Significant reductions ($p < 0.005$) of Zinquin fluorescence were seen in a range of mast cells (CBMC, bone marrow-derived human mast cells, RPMC, immature and mature HMC-1 cells) treated with various degranulators (1 μg/ml compound 48/80, 0.5 μg/ml IgE + 0.2 μM anti-IgE, and 100 nM PMA + 0.5 μM A23187); these reductions in Zinquin fluorescence were of a similar magnitude to the decreases induced by the Zn chelator TPEN (Table I).

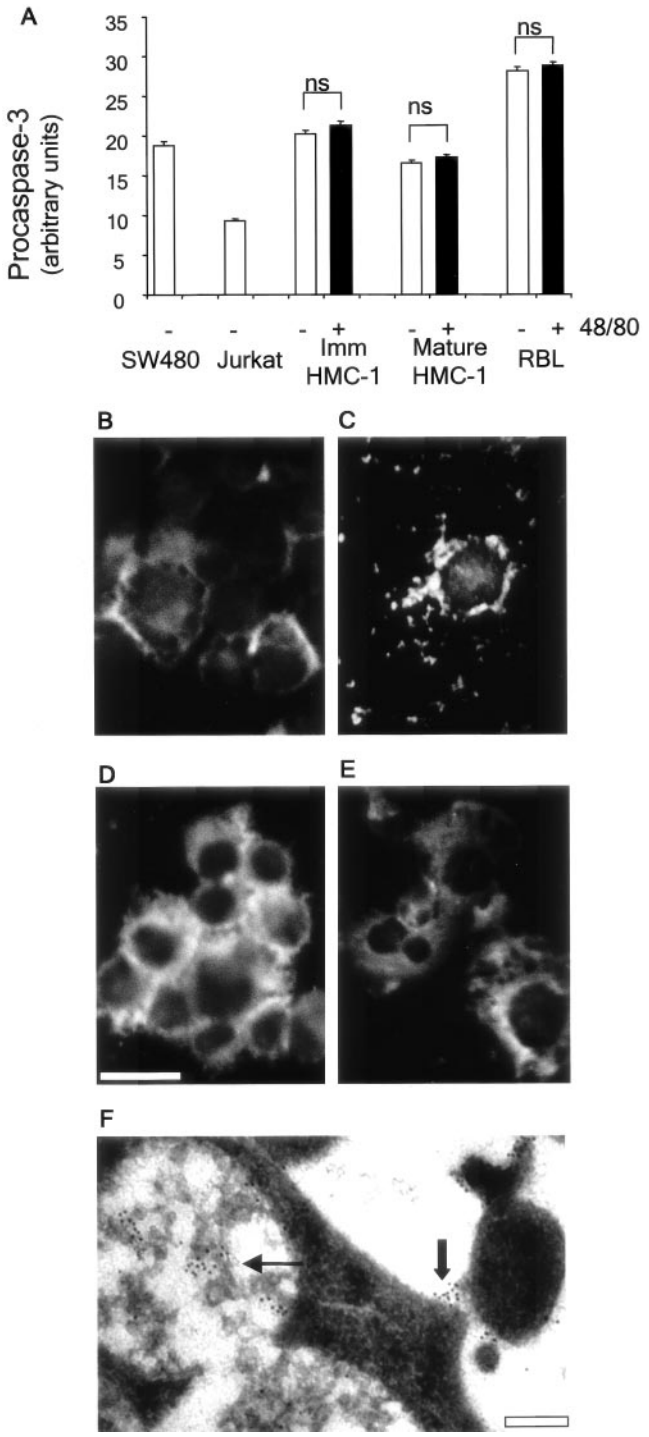

FIGURE 3. Expression and subcellular localization of procaspase-3 in immature and mature HMC-1 cells treated with compound 48/80. *A*, Graph showing quantification of Northern blot analysis using a procaspase-3 probe Figure shows high expression of procaspase-3 mRNA in immature HMC-1 mast cells and no variation with activation by compound 48/80. Positive control was mRNA from high procaspase-3-expressing SW620 cells; extracts from a low-expressing cell line Jurkat are included for comparison. Loading controls consisted of parallel ethidium bromide staining of 18S rRNA bands. *B–E*, Shows four typical confocal images of procaspase-3 localization in immature (*B* and *C*) and mature (*D* and *E*) HMC-1 cells before (*B* and *D*) and after (*C* and *E*) treatment with 1 μg/ml compound 48/80. Scale bar indicates 20 μm. *F*, Shows clusters of gold-labeled procaspase-3 associated with amorphous material within typical granules (thin filled arrow) of mature HMC-1 cell. Note also the presence of procaspase-3 labeling in exocytosed material (thick filled arrow). Scale bar indicates 200 nm.

Repletion of Zn after degranulation

To investigate whether mast cells can replete their Zn stores following degranulation, mature HMC-1 cells were degranulated with 1 μg/ml compound 48/80 for 18 h, then washed and cultured in fresh medium for 24 h, and Zinquin fluorescence was again measured. Zinquin fluorescence decreased from 79.9 $\pm$ 4.1 GSU in control cells to 38.5 $\pm$ 4.2 in cells treated with compound 48/80 ($p < 0.005$). After reculture, Zinquin fluorescence was 73.8 $\pm$ 3.7 GSU, not significantly different from the initial Zinquin fluorescence of the untreated mast cells.

Localization and levels of ZnT_4 in mast cells

To further investigate the mechanism of Zn repletion in mast cells, we looked at the expression of a major cellular Zn transporter, ZnT_4. RT-PCR showed the presence of ZnT_4 mRNA in untreated mature HMC-1, immature HMC-1, and RBL-2H3 cells. The 1.2-kb fragment can only be the result of cDNA amplification, because the primers we have used for ZnT_4 PCR would amplify a much larger fragment on genomic DNA, due to the long introns that are present in the ZnT_4 gene (15).

The levels were greater than those of rat kidney and comparable to those of rat intestine, tissues that express relatively high levels of this transporter (Fig. 1*I*). Because it is known that changes in Zn homeostasis in some types of cell can lead to up- or down-regulation of Zn transporter gene expression (9), it was therefore of interest to determine whether the marked changes in Zn levels in degranulating mast cells can also affect expression of one of its Zn transporters. Northern blotting showed no significant change in ZnT_4 mRNA expression in immature HMC-1 cells before and after degranulation. In a typical experiment in which band intensity was quantified by phosphor imaging, the mean intensity of the band was 10.1 $\pm$ 0.6 arbitrary units ($n = 3$) in untreated cells and 8.5 $\pm$ 0.7 in compound 48/80-treated cells (not significant). Similar results were seen for mature HMC-1 and RBL-2H3 mast cells (data not shown).

High levels of ZnT_4 in mast cells were also shown by strong immunocytochemical labeling with rabbit anti-ZnT_4 in paraformaldehyde-fixed, Triton X-100-permeabilized HMC-1 cells. Like Zinquin labeling, the fluorescence was cytoplasmic, and often granular-like in distribution. Dual labeling confocal studies in mature HMC-1 cells showed little colocalization of immunoreactive ZnT_4 (green) and Zinquin-labeled Zn (red) (Fig. 1*J*), suggesting that they are contained in different subsets of vesicles/granules. There was little overlap, as indicated by lack of orange in the merged image. ZnT_4 had a vesicular-like pattern of fluorescence both in the cytoplasm and around the nucleus (Fig. 2, *A* and *B*). There was no significant decrease in ZnT_4 immunofluorescence following degranulation with compound 48/80 in either immature (Fig. 2, *A* and *B*) or mature HMC-1 cells (data not shown), although a significant decrease did occur in RPMC cells treated with compound 48/80 (Fig. 2, *C* and *D*). Thus, for compound 48/80-treated immature HMC-1 cells, the levels of ZnT_4 fluorescence were 102.1 $\pm$ 1.6% of those before degranulation (not significant); for mature HMC-1 cells, they were 97.8 $\pm$ 1.6% (not significant), while for RPMC they were 72.9 $\pm$ 1.4% ($p < 0.005$). The decrease in ZnT_4 levels following activation of RPMC is consistent with a granular localization for this transporter. RPMC, which are rich in secretory granules, often had a pronounced apical and granular-like fluorescence (Fig. 2*C*).

The localization of ZnT_4 in immature and mature HMC-1 was also examined by electron microscopy using immunogold labeling. In immature HMC-1 cells (Fig. 2, *E* and *F*), gold particles labeling ZnT_4 were observed in the apical cytoplasm near and within the plasma membranes (Fig. 2*E*, thin arrow) as well as inside the granules and in proximity to the granule membranes (Fig. 2*F*, thick

arrows). Similar patterns were seen with mature HMC-1 cells. There was a mean of 7.9 ± 0.6 particles per granule in immature HMC-1 cells and 6.0 ± 0.5 in mature HMC-1 cells (not significant). There was negligible labeling in the cells not treated with primary Ab (0.13 ± 0.1 particles per granule). When data were corrected for granular area, significant differences were seen between the counts for ZnT_4-labeled immature HMC-1 cells with 69.5 ± 8.0 gold particles per μm^2 of granule compared with 98.8 ± 8.6 gold particles per μm^2 of granule ($p < 0.05$).

Expression of procaspase-3 in mast cells

Procaspase-3 mRNA was detected by Northern blotting and quantified by phosphor imaging (Fig. 3*A*). There was no effect of compound 48/80 on the levels of procaspase-3 mRNA with untreated immature HMC-1 cells having a mean band intensity (arbitrary units) of 20.3 ± 0.4 compared with 21.3 ± 0.5 after treatment for 18 h with 1 μg/ml compound 48/80 (not significant). Similar results were obtained for mature HMC-1 cells and RBL-2H3 cells (data not shown).

Immunofluorescence confocal labeling in immature and mature HMC-1 cells showed moderate levels of procaspase-3 with a vesicular-like distribution, similar to that of Zn (Fig. 3, *B* and *D*). Mean fluorescence decreased in cells treated with compound 48/80 (Fig. 3, *C* and *E*; Table II), consistent with a localization of procaspase-3 in secretory granules. Similar results were seen for procaspase-4 (Table II).

The localization of procaspase-3 distribution was further studied using an immunogold technique. Fig. 3*F* shows immunogold labeling of procaspase-3 in immature HMC-1 cells, which was especially prominent in the amorphous material of mast cell granules (thin arrows) and in exocytosed material (thick arrow). As expected, controls lacking primary Ab were not stained (data not shown).

Effects of Zn depletion on procaspase-3 activation

To determine effects of Zn depletion on susceptibility of mast cells to undergo apoptosis, immature HMC-1 cells were depleted of Zn by two strategies. In the first method, Zn was functionally depleted by chelation with TPEN; in the second method, Zn was depleted by degranulation. These treatments were done either in the absence or presence of a suboptimal concentration of the apoptotic inducer sodium butyrate. Active caspase-3 levels were measured in cell lysates using the fluorogenic substrate DEVD-AFC.

Fig. 4 shows that butyrate induced a concentration-dependent increase in caspase-3 activity (Fig. 4*A*), at concentrations beyond those require to induce maturation. At the highest concentration of butyrate tested (10 mM), caspase-3 activity increased 4.6 ± 0.7-fold over that of untreated HMC-1 cells.

Functional Zn depletion by chelation with TPEN also induced caspase-3 activity in immature HMC-1 cells in a concentration-dependent manner (Fig. 4*B*). At the highest concentration of TPEN tested (100 μM), caspase-3 activity increased 4.3 ± 1.1-fold over that of untreated HMC-1 cells. A synergistic interaction of suboptimal concentrations of butyrate (2 mM) and TPEN (25 μM) was observed (Fig. 4*C*), with a combination of the reagents inducing an 11.1 ± 1.0-fold increase in caspase-3 activity, compared with an expected increase of 5.4-fold (dotted line in Fig. 4*C*), if the interaction was additive ($p < 0.005$).

In contrast to this effect of TPEN, degranulators did not induce caspase activation by themselves. Nor did they synergize with butyrate. Thus, a combination of 2 mM butyrate and either compound 48/80 (1 μg/ml) or PMA (100 nM) + A23187 (0.5 μM) did not increase caspase-3 levels over those induced by 2 mM butyrate alone (Fig. 4*C*). These results were typical of four experiments. This was despite the level of Zinquin-stainable Zn falling to the same level as in TPEN-treated cells (Table I). Similar results were found for mature HMC-1 cells and CBMC.

To determine whether these different effects of TPEN and degranulators on caspase activation were also seen with morphological changes of apoptosis, chromatin fragmentation was assayed using Hoechst 3342. Fig. 4, *D–F*, shows typical images of the Hoechst 33342-stained cells in untreated (Fig. 4*D*), compound 48/80 treated (Fig. 4*E*), and TPEN treated (Fig. 4*F*). Although TPEN was able to induce apoptosis, the mast cell activator compound 48/80 did not. Untreated cells contained 7.2% apoptotic cells, and there was no increase in compound 48/80-treated cells. In contrast, TPEN induced 87% apoptosis, which included 45% early apoptotic cells and 42% fragmented cells.

Effects of Zn depletion and supplementation on NF-κB activation

Nuclear translocation of NF-κB and altered gene expression most likely regulate granulocyte apoptosis (18). The next experiment

Table II. *Effect of degranulation on procaspase-3 and procaspase-4 levels*

	Caspase-3				Caspase-4			
Cells	Expt. 1	Expt. 2	Expt. 3	Mean[d]	Expt. 1	Expt. 2	Expt. 3	Mean[d]
Immature HMC-1								
Control[a]	23.6 ± 0.5	39.9 ± 0.8	39.9 ± 0.4	34.5	34.3 ± 0.8	26.4 ± 0.7	30.2 ± 0.6	30.3
+48/80[b]	15.5 ± 0.3**	11.6 ± 0.3**	14.8 ± 0.3**	14.0	25.8 ± 0.7**	6.5 ± 0.2**	16.4 ± 0.6**	16.2
n[c]	347	355	321		340	273	219	
Mature HMC-1								
Control[a]	20.2 ± 0.3	46.4 ± 1.2	52.0 ± 0.9	39.6	36.3 ± 1.2	37.0 ± 1.4	46.4 ± 1.1	39.9
+48/80[b]	15.8 ± 0.2**	17.1 ± 0.5**	17.7 ± 0.9**	16.8	7.6 ± 0.4**	17.0 ± 0.5**	14.7 ± 0.5**	13.1
n[c]	484	283	109		272	121	213	
RPMC								
Control[a]	42.0 ± 1.5	38.3 ± 1.1	41.6 ± 0.7	40.6	28.1 ± 0.7	12.5 ± 0.5		20.3
+48/80[b]	27.9 ± 1.6**	27.1 ± 1.6**	14.2 ± 0.4**	23.1	6.0 ± 0.3**	10.4 ± 0.5**		8.2
n[c]	144	190	224		233	128		

[a] Mean procaspase fluorescence of untreated cells for individual experiments ± SEM (GSU).
[b] Mean procaspase fluorescence of cells treated for 18 h with 1 μg/ml compound 48/80 for individual experiments ± SEM (GSU).
[c] Total number of cells used for quantification of fluorescence.
[d] Mean of individual experiments.
**, $p < 0.005$.

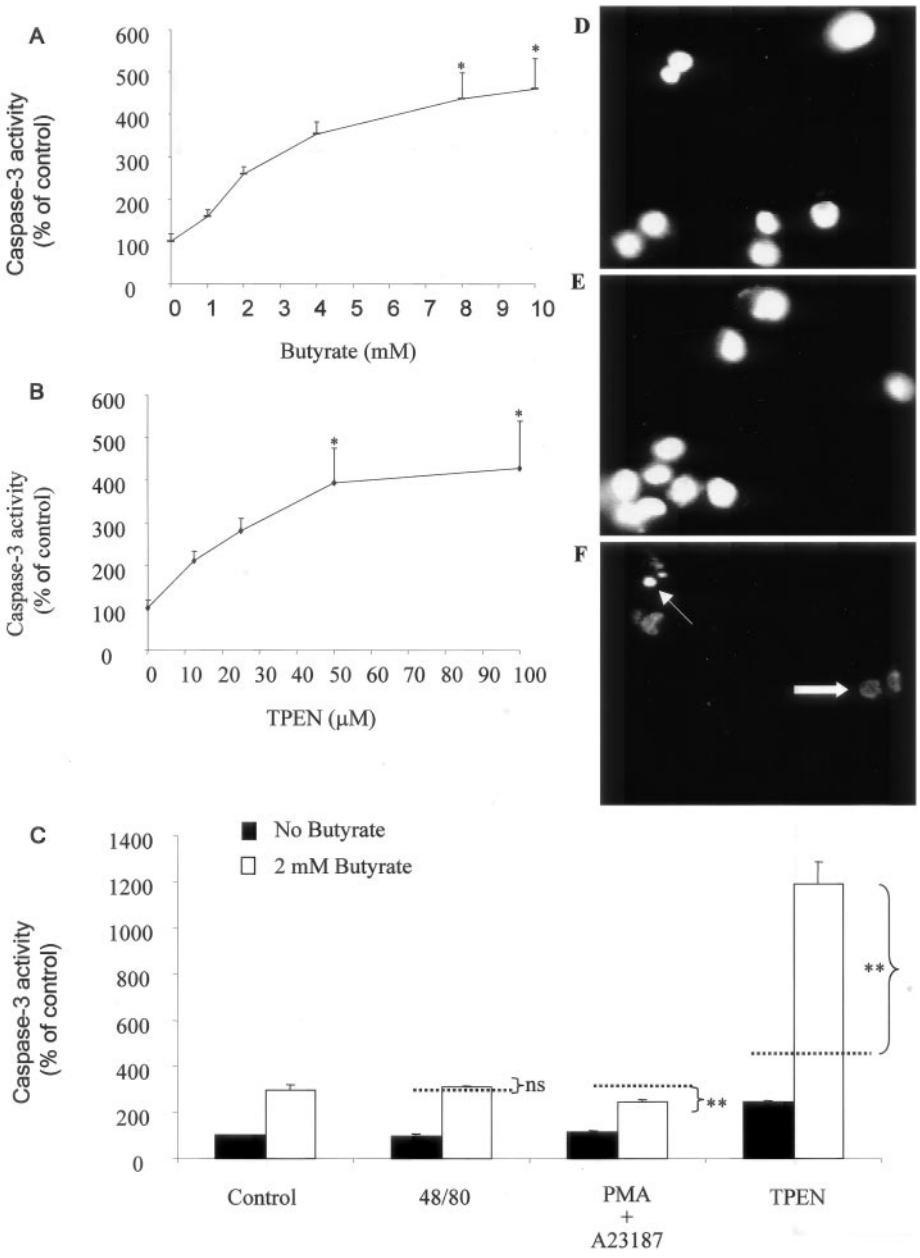

FIGURE 4. Effect of degranulation or Zn chelation on caspase-3 activity and apoptosis. Figure shows synergistic increases in caspase-3 activity between butyrate and TPEN in immature HMC-1 cells, but no synergy between degranulators and butyrate. *A*, Concentration-dependent induction of caspase-3 activity by butyrate. Immature HMC-1 cells were treated with butyrate for 18 h. Cells were then assayed for caspase-3 activity, expressed as percentage of that in control cells (no butyrate). *B*, Concentration-dependent induction of caspase-3 activity by TPEN. Immature HMC-1 cells were treated with TPEN for 18 h. Cells were then assayed for caspase-3 activity, expressed as percentage of that in control cells (no TPEN). *C*, Interactions between butyrate and degranulators or TPEN in induction of caspase-3 activity. Immature HMC-1 cells were treated with degranulators (1 μg/ml compound 48/80 or 100 nM PMA + 0.5 μM A23187) or 25 μM TPEN, in the presence (■) or absence (□) of 2 mM butyrate, for 18 h. Cells were then assayed for caspase-3 activity, expressed as percentage of that in control cells (no treatment). Dotted lines show expected values if interactions are additive. Note the synergistic interaction between TPEN and butyrate, but lack of synergy between degranulators and butyrate. Data are means of triplicates ± SEM for a typical experiment. Control levels were 1.4 ± 0.04 caspase-3 U/mg protein/h. *D–F*, Typical images of Hoechst dye 33342-stained immature HMC-1 mast cells showing minimal apoptosis in control (*D*) and compound 48/80-treated cells (*E*). By contrast, TPEN-treated cells (*F*) showed typical fragmentation of chromatin (thin arrow) and condensation of chromatin around rim of nucleus (thick arrow).

was to determine whether intracellular Zn regulated NF-κB activation. Untreated immature HMC-1 mast cells were positive by immunofluorescence (quantified by image analysis; Fig. 5*A*) and had a typical cytoplasmic fluorescence for NF-κB (Fig. 5*B*, *upper left* and *middle panels*). As a positive control, immature HMC-1 mast cells were treated with 20 ng/ml TNF-α. There was a marked redistribution of NF-κB to the nucleus seen in 92.8% of the cells (Fig. 5*B*, *bottom left* and *middle panels*). There was also a small percentage (3.6%) of cells in the TNF-α-treated population displaying a perinuclear localization of NF-κB. This redistribution was accompanied by an increase in total cellular fluorescence for NF-κB (Fig. 5*A*, □, $p < 0.005$). Zn supplementation prevented both the increase in total cellular fluorescence (Fig. 5*A*, ■) and nuclear translocation of NF-κB (Fig. 5*B*, *lower right panel*). These results were identical with those obtained for mature HMC-1 and RBL-2H3 cells (data not shown).

In these experiments, Zn was supplemented in cells by addition of 25 μM $ZnSO_4$ plus the Zn ionophore sodium pyrithione. Treatment of mast cells in this way increased intracellular Zn levels of HMC-1 cells and CBMC by 31.7% (SEM 9.5%, $p < 0.05$) and 53.3% (SEM 7.3%, $p < 0.05$), respectively. Increase in fluorescence was seen in both cytoplasmic and nuclear compartments. To ensure that pyrithione itself was not having a direct effect on NF-κB or being cytotoxic for the mast cells, an experiment was performed with various concentrations of pyrithione (0.1, 0.5, 1, 2, and 4 μM) in the absence of exogenous Zn. There was no effect on either activation of NF-κB or viability of HMC-1 cells at 0.1 μM pyrithione, which was the concentration used in the Zn supplementation studies. However, there was toxicity at concentrations greater than 1 μM pyrithione.

These experiments were then extended to determine whether Zn depletion by 25 μM TPEN would influence activation of NF-κB. There was a redistribution of NF-κB fluorescence to the nucleus from the cytoplasm in 70.9% of the cells and perinuclear redistribution in 22.3% of the cells (Fig. 5*B*; Table III). Zn supplementation prevented the redistribution to the nucleus (Table III) and the increase in total cellular fluorescence (Fig. 5*A*, $p < 0.005$). Similar results were obtained for TPEN-treated mature HMC-1

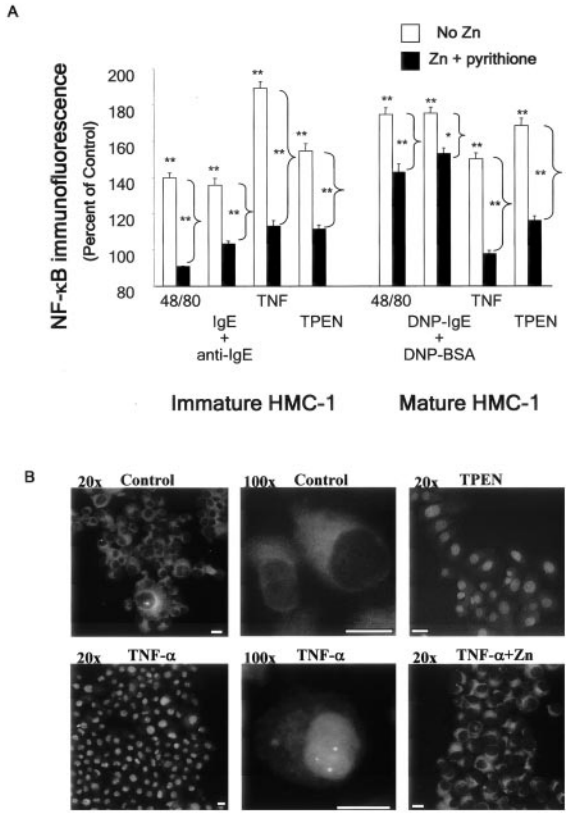

FIGURE 5. Effect of TNF-α, TPEN, or degranulators on NF-κB immunofluorescence in HMC-1 mast cells with and without Zn supplementation. *A*, Immature or mature HMC-1 mast cells were treated with 25 μM $ZnSO_4$ and 0.1 μM pyrithione for 30 min to increase intracellular Zn (■). Cells were then treated with 20 ng/ml TNF-α for 2 h, or 25 μM TPEN for 4 h, or degranulators for 18 h. Some cells were treated with these agents without Zn supplementation (open columns). Figure shows an increase in total cellular NF-κB immunofluorescence in cells treated with all agents and significant decreases in fluorescence of NF-κB following Zn supplementation. Data are expressed as percentage of controls and are means of triplicates ± SEM for a typical experiment. Statistical significances are indicated as: *, $p < 0.05$; **, $p < 0.005$. Asterisks on top of the columns indicate comparison with untreated (control) cells. Asterisks on side of the columns indicate comparison between nonsupplemented and Zn-supplemented cells. *B*, Typical images are shown; note the cytoplasmic fluorescence in control and Zn-supplemented cells and nuclear fluorescence in TPEN- and TNF-treated cells. Scale bars indicate 20 μm for all panels.

mast cells and TPEN-treated RBL-2H3 mast cells (data not shown). Thus, the level of intracellular Zn negatively influences the translocation of NF-κB to the nucleus.

To determine whether Zn depletion by degranulation had similar effects to that of TPEN, mast cells were treated with compound 48/80, IgE/anti-IgE, or for rat mast cells DNP-IgE/DNP-BSA, the equivalent of IgE/anti-IgE for human mast cells. There was an increase in total cellular NF-κB fluorescence for immature HMC-1 cells treated with each of the degranulators (Fig. 5*A*, $p < 0.005$). This was associated with a small increase in perinuclear staining. Similar results were seen for mature HMC-1 cells, except that there was a greater increase in perinuclear staining and a moderate increase in nuclear staining (data not shown). The one major difference between the mast cell types was that for mature HMC-1 cells, degranulators gave an equivalent effect to treatment with TNF-α and TPEN, whereas with the other mast cell types degranulators had significantly less effect. Zn supplementation decreased total cellular NF-κB fluorescence for each mast cell type ($p < 0.005$).

Discussion

The major finding in this study was the presence of labile Zn, ZnT_4, and procaspases in the granules of mast cells. We have used a number of mast cell types in these experiments because we wanted to investigate the responses of various mast cell types, both primary and cell lines from mice and humans, as well as to test the generality of the observations.

The observation that mast cells can be cultured for long periods in the same low Zn-containing medium as other cells (e.g., A549 cells), and yet contain much more Zn, implies that mast cells have a well-developed mechanism for uptake of this metal ion as well as mechanisms to concentrate Zn into secretory granules. Recent studies in pancreatic islet cells suggest that their high content of Zn in secretory granules is due to localization of the Zn transporter ZnT_5 in the membranes of these granules (13). In this study, we show high expression of ZnT_4 mRNA and protein in at least two different types of mast cell, HMC-1 and RBL-2H3. ZnT_4 had a granular distribution like that of Zinquin labeling and may enable mast cells to scavenge extra Zn from their environment more readily than other cells, particularly after activation and degranulation. The partial colocalization of Zn- and ZnT_4-positive vesicles suggests that ZnT_4 is lost from granule membranes when they have accumulated sufficient Zn. Alternatively, ZnT_4-containing vesicles may be less readily involved in the secretory pathway and more involved in endocytic pathways. Although degranulation with compound 48/80 did not decrease levels of ZnT_4 in HMC-1 cells, it did significantly reduce levels of ZnT_4 in RPMC, indicating a difference in the disposition of this transporter in these primary cells. There may be a degree of selectivity in the types of secretory products released in response to a given signal. Immunogold localization of ZnT_4 following degranulation may prove useful in further analysis of the distribution of ZnT_4 between intra- and extragranular locations, particularly in RPMC, in which there are more, and better developed, secretory granules. There is still much debate concerning which intracellular pools of labile Zn are detected by Zinquin. Within granules, the bulk probably exists in loose association with secretory products, as has been shown for pancreatic islets, in which Zinquin detects the Zn bound to insulin (30).

There are several explanations for the presence of procaspases in mast cell granules. First, they may be released and activated during degranulation and cleave extracellular substrates, such as matrix proteins. There is as yet no evidence that extracellular proteins can serve as substrates for caspases. Second, released caspases might induce apoptosis in neighboring cells, in the same way that smooth muscle cells undergo apoptosis in response to chymase released from mast cell granules (32). Finally, granular caspases may have a special function in cleaving proteins within the granules. It should be stressed in this work that we do not believe that intragranular caspases trigger cell apoptosis. Rather, they may act secondarily to the apoptotic cascade, facilitating the cleavage of intragranular proteins. Because labile Zn is an inhibitor of procaspase activation, mast cell granule Zn may play a role in the regulation of granule procaspases, and ZnT_4 may regulate the levels of granular Zn.

In this study, it was shown that there were no increases in active caspase-3 levels or apoptosis of mast cells following treatment with mast cell activators, supporting other evidence (3) that mast cells do not die by apoptosis as a result of activation and degranulation. If procaspases are located in the granules of mast cells and are released during degranulation, one would predict that the apoptotic response of degranulated cells to a toxin would be diminished. To some extent this was observed, because cells treated with a combination of degranulator and either butyrate or staurosporine

Table III. *Localization of NF-κB in immature HMC-1 cells*

Conditions[a]	*n*	% Cytoplasmic[b]	% Perinuclear	% Nuclear	% Nuclear + % Perinuclear
Untreated	361	100 ± 0.0	0.0 ± 0.0	0.0 ± 0.0	0.0 ± 0.0
48/80	350	92.0 ± 2.3	8.0 ± 2.3	0.0 ± 0.0	8.0 ± 2.3
48/80 + Zn	342	95.9 ± 0.6	4.1 ± 0.6	0.0 ± 0.0	4.1 ± 0.6
IgE/Anti-IgE	217	92.1 ± 3.1	6.0 ± 3.3	2.0 ± 2.0	7.9 ± 3.1
IgE/Anti-IgE + Zn	329	97.3 ± 0.4	2.7 ± 0.4	0.0 ± 0.0	2.7 ± 0.4
TNF-α	391	3.6 ± 3.6**	3.6 ± 0.7	92.8 ± 2.9**	96.4 ± 3.6**
TNF-α + Zn	318	97.4 ± 2.6**	2.6 ± 2.6	0.0 ± 0.0**	2.6 ± 2.6**
TPEN	372	6.8 ± 0.3**	22.3 ± 0.9**	70.9 ± 1.1**	93.2 ± 0.3**
TPEN + Zn	345	87.1 ± 5.4**	5.8 ± 3.6*	7.2 ± 3.0**	12.9 ± 5.4**

[a] Cells were treated with 48/80 (1 μg/ml, 18 h), IgE (5 μg/ml for 18 h), followed by anti-IgE (1/5000 for 2 h), TNF (20 ng/ml for 4 h), or no addition (for 18 h).
[b] Data are expressed as percentage of total (mean ± SEM).
* One-way ANOVA analysis was used in conjunction with the post hoc Tukey HSD test, $p < 0.05$ and **, $p < 0.005$: asterisks alongside SEM indicate comparisons between untreated and corresponding treated cells for each pattern of labeling, while those beneath the SEM refer to comparisons between with and without Zn treatment.

had less caspase activity than would be predicted if these two toxins were having a simple additive effect.

A major conclusion from these experiments is that there are two distinct pools of labile Zn in mast cells. First, there is the pool that is contained within the granules and is released during mast cell activation. This pool is unlikely to play an important role in the regulation of mast cell apoptosis, because in cells in which Zn was depleted by degranulation, these cells were no more susceptible to an apoptotic inducer than those that still contained granular Zn. The second pool of labile Zn, which is depleted by TPEN, is involved in the regulation of caspases because TPEN-treated cells were more susceptible to an apoptotic inducer (e.g., butyrate) than those cells not treated with TPEN. It was difficult to study the locations of the antiapoptotic pools of Zn in these cells using Zinquin fluorescence due to the abundance of Zn in the granules. The localization of extragranular Zn may be better studied in mast cells at the electron microscopic level by the autometallography technique (33).

The results with NF-κB showed that modulation of intracellular Zn levels can strongly influence its translocation to the nucleus, suggesting it may regulate gene expression. It is not clear whether in mast cells NF-κB is proapoptotic or antiapoptotic. Some studies have suggested that NF-κB promotes apoptosis due to its involvement in the expression of proapoptotic genes, including TNF-α, c-*myc*, and Fas ligand, while other studies have shown that NF-κB increases expression of antiapoptotic factors, including cytoplasmic inhibitors of apoptosis, TNFR-associated factors, and Bcl-2 homologues (34). The finding that Zn prevented the activation and translocation of NF-κB in each mast cell type confirms the findings of Connell et al. (35) in endothelial cells, a noninflammatory cell type. The action of Zn in the inhibition of NF-κB activation has not been defined. One possibility is that Zn blocks the phosphorylation of I-κB-α, thereby preventing the translocation of NF-κB into the nucleus (36). Another way in which Zn might inhibit NF-κB translocation is through its suppression of caspase-3, which cleaves I-κB-α in vitro (37).

There are no known physiological modulators of intracellular Zn levels. A better understanding of how Zn uptake and efflux transporters function should lead to the identification of such inducers. The whole area of Zn transporter research is moving quickly, and their functional roles, as well as changes in disease states, are subjects that will receive a lot of attention. As Abs and probes become available, it will be possible to study the relationship of other Zn transporters to mast cell Zn homeostasis. The implications of activation-associated changes in intracellular Zn for mast cell function and turnover now require better understanding in the context of both normal and pathological conditions (e.g., asthma). Clarification of the functions of labile Zn within mast cells, the mechanisms of uptake and subcellular redistribution, and the types of mast cell granule proteins (heparin, procaspase-3, or mast cell proteases) with which Zn interacts should begin to address questions concerning the significance of this metal ion in mast cell biology.

Acknowledgments

We thank Joseph Butterfield (Mayo Clinic and Foundation) for his kind gift of HMC-1 cells, Dr. Leonie Ashman (Hanson Centre for Cancer Research, Adelaide, Australia) for providing the YB5.B8 mAb, Dr. Russell Ludowyke (St. Vincent's Hospital), Rachel Gibson (Royal Adelaide Hospital, Adelaide, Australia) for her assistance with animal studies, and Scott Townley (Flinders Medical Centre, Bedford, Australia) for the protocol for isolating rat peritoneal mast cells. We are grateful to Dr. Meredith Wallwork (Waite Institute, Adelaide, Australia) for her assistance with confocal studies, and Lyn Waterhouse (Adelaide Microscopy, University of Adelaide) for electron microsocopy studies.

References

1. Holgate, S., and M. Church. 1992. The mast cell. *Br. Med. Bull. 48:40*.
2. Metcalfe, D., D. Bram, and Y. Mekori. 1997. Mast cells. *Physiol. Rev. 77:1033*.
3. Dvorak, A., R. Schleimer, and L. Lichtenstein. 1988. Human mast cells synthesize new granules during recovery from degranulation: in vitro studies with mast cells purified from human lungs. *Blood 71:76*.
4. Gustafson, G. 1967. Heavy metals in rat mast cell granules. *Lab. Invest. 17:588*.
5. Zalewski, P. D., I. J. Forbes, and W. H. Betts. 1993. Correlation of apoptosis with change in intracellular labile Zn, using Zinquin, a new specific fluorescent probe for zinc. *Biochem. J. 296:403*.
6. Zalewski, P., I. Forbes, R. Seamark, R. Borlinghaus, H. Betts, S. Lincoln, and A. Ward. 1994. Flux of intracellular labile zinc during apoptosis (gene-directed cell death) revealed by a specific chemical probe, Zinquin. *Chem. Biol. 1:153*.
7. Truong-Tran, A., D. Grosser, R. Ruffin, C. Murgia, and P. Zalewski. 2003. Apoptosis in the normal and inflamed airway epithelium: role of zinc in epithelial protection and procaspase-3 regulation. *Biochem. Pharmacol. 66:1459*.
8. Ho, L., R. Ratnaike, and P. Zalewski. 2000. Involvement of intracellular labile zinc in suppression of DEVD-caspase activity in human neuroblastoma cells. *Biochem. Biophys. Res. Commun. 268:148*.
9. Kambe, T., Y. Yamaguchi-Iwai, R. Sasaki, and M. Nagao. 2004. Overview of mammalian zinc transporters. *Cell. Mol. Life Sci. 61:49*.
10. Murgia, C., I. Vespignani, J. Cerase, F. Nobili, and G. Perozzi. 1999. Cloning, expression, and vesicular localization of zinc transporter Dri 27/ZnT4 in intestinal tissue and cells. *Am. J. Physiol. 277:G1231*.
11. Gaither, L., and D. Eide. 2001. The human ZIP1 transporter mediates zinc uptake in human K562 erythroleukemia cells. *J. Biol. Chem. 276:22258*.
12. Palmiter, R., T. Cole, C. Quaife, and S. Findley. 1996. ZnT-3, a putative transporter of zinc into synaptic vesicles. *Proc. Natl. Acad. Sci. USA 93:14924*.
13. Kambe, T., H. Narita, Y. Yamaguchi-Iwai, J. Hirose, T. Amano, N. Sugiura, R. Sasaki, K. Mori, T. Iwanaga, and M. Nagao. 2002. Cloning and characterization of a novel mammalian zinc transporter, zinc transporter 5, abundantly expressed in pancreatic β cells. *J. Biol. Chem. 277:19049*.
14. Cragg, R., G. Christie, S. Phillips, R. Russi, S. Kury, J. Mathers, P. Taylor, and D. Ford. 2002. A novel zinc-regulated human zinc transporter, hZTL1, is localized to the enterocyte apical membrane. *J. Biol. Chem. 277:22789*.
15. Huang, L., and J. Gitschier. 1997. A novel gene involved in zinc transport is deficient in lethal milk mouse. *Nat. Genet. 17:292*.

16. Ranaldi, G., G. Perozzi, A. Truong-Tran, P. Zalewski, and C. Murgia. 2002. Intracellular distribution of labile Zn (II) and zinc transporter expression in the kidney and in MDCK cells. *Am. J. Physiol. Renal Physiol. 283:F1365*.
17. Lee, J., and F. Burckart. 1998. Nuclear factor κB: important transcription factor and therapeutic target. *J. Clin. Pharmacol. 38:981*.
18. Ward, C., E. Chilvers, M. Lawson, J. Pryde, S. Fujihara, S. Farrow, C. Haslett, and A. Rossi. 1999. NF-κB activation is a critical regulator of human granulocyte apoptosis in vitro. *J. Biol. Chem. 274:4309*.
19. Karin, M. 1998. The NF-κB activation pathway: its regulation and role in inflammation and cell survival. *Cancer J. Sci. Am. 4:S92*.
20. Wang, J., and M. Lenardo. 2000. Roles of caspases in apoptosis, development, and cytokine maturation revealed by homozygous gene deficiencies. *J. Cell Sci. 113:753*.
21. Butterfield, J., D. Weiler, G. Dewald, and G. Gleich. 1988. Establishment of an immature mast cell line from a patient with mast cell leukemia. *Leuk. Res. 12:345*.
22. Galli, S., A. Dvorak, J. Marcum, T. Ishizaka, G. Nabel, H. Der Simonian, K. Pyne, J. Goldin, R. Rosenberg, H. Cantor, and H. Dvorak. 1982. Mast cell clones: a model for the analysis of cellular maturation. *J. Cell Biol. 95:435*.
23. Medina, V., B. Edmonds, G. Young, R. James, S. Appleton, and P. Zalewski. 1997. Induction of caspase-3 protease activity and apoptosis by butyrate and trichostatin A (inhibitors of histone deacetylase): dependence on protein synthesis and synergy with a mitochondrial/cytochrome *c*-dependent pathway. *Cancer Res. 57:3697*.
24. Lieber, M., B. Smith, A. Szakal, W. Nelson-Rees, and G. Todaro. 1976. A continuous tumor-cell line from a human lung carcinoma with properties of type II alveolar epithelial cells. *Int. J. Cancer 17:62*.
25. Yamaguchi, M., K. Sayama, K. Yano, C. Lantz, N. Noben-Trauth, C. Ra, J. Costa, and S. Galli. 1999. IgE enhances Fce receptor I expression and IgE-dependent release of histamine and lipid mediators from human umbilical cord blood-derived mast cells: synergistic effect of IL-4 and IgE on human mast cell Fce receptor I expression and mediator release. *J. Immunol. 162:5455*.
26. Okayama, Y., T. Hunt, O. Kassel, L. Ashman, and M. Church. 1994. Assessment of the anti-c-*kit* monoclonal antibody YB5.B8 in affinity magnetic enrichment of human lung mast cells. *J. Immunol. Methods 169:153*.
27. Li, L., J. Macpherson, S. Adelstein, C. Bunn, K. Atkinson, K. Phadke, and S. Krilis. 1995. Conditioned media from a cell strain derived from a patient with mastocytosis induces preferential development of cells that possess high affinity IgE receptors and the granule protease phenotype of mature cutaneous mast cells. *J. Biol. Chem. 270:2258*.
28. Arslan, P., F. Di Virgilio, M. Beltrame, R. Y. Tsien, and T. Pozzan. 1985. Cytosolic Ca^{2+} homeostasis in Ehrlich and Yoshida carcinomas: a new, membrane-permeant chelator of heavy metals reveals that these ascites tumor cell lines have normal cytosolic free Ca^{2+}. *J. Biol. Chem. 260:2719*.
29. Jasim, S., and H. Tjalve. 1986. Effects of sodium pyridinethione on the uptake and distribution of nickel, cadmium and zinc in pregnant and non-pregnant mice. *Toxicology 38:327*.
30. Zalewski, P. D., S. H. Millard, I. J. Forbes, O. Kapaniris, A. Slavotinek, and W. H. Betts. 1994. Video image analysis of labile zinc in viable pancreatic islet cells using a specific fluorescent probe for zinc. *J. Histochem. Cytochem. 42:877*.
31. Mio, M., M. Yabuta, and C. Kamei. 1999. Ultraviolet B (UVB) light-induced histamine release from rat peritoneal mast cells and its augmentation by certain phenothiazine compounds. *Immunopharmacology 41:55*.
32. Leskinen, M., Y. Wang, D. Leszczynski, K. Lindstedt, and P. Kovanen. 2001. Mast cell chymase induces apoptosis of vascular smooth muscle cells. *Arterioscler. Thromb. Vasc. Biol. 21:516*.
33. Danscher, G., J. Obel, and O. Thorlacius-Ussing. 1980. Electron microscopic demonstration of metals in rat mast cells: a cytochemical study based on an improved sulphide silver method. *Histochemistry 66:293*.
34. Aggarwal, B. 2000. Apoptosis and nuclear factor-κB: a tale of association and dissociation. *Biochem. Pharmacol. 60:1033*.
35. Connell, P., V. Young, M. Toborek, D. Cohen, S. Barve, C. McClain, and B. Hennig. 1997. Zinc attenuates tumor necrosis factor-mediated activation of transcription factors in endothelial cells. *J. Am. Coll. Nutr. 16:411*.
36. Jeon, K., J. Jeong, and D. Jue. 2000. Thiol-reactive metal compounds inhibit NF-κB activation by blocking IκB kinase. *J. Immunol. 164:5981*.
37. Barkett, M., D. Xue, H. Horvitz, and T. Gilmore. 1997. Phosphorylation of IκBa inhibits its cleavage by caspase CPP32 in vitro. *J. Biol. Chem. 272:29419*.